Spectrally Resolved Dynamics of Energy Transfer in Quantum-Dot Assemblies: Towards Engineered Energy Flows in Artificial Materials

S. A. Crooker, J. A. Hollingsworth, S. Tretiak, and V. I. Klimov
Los Alamos National Laboratory, Los Alamos, New Mexico 87545
(Received 4 June 2002; published 14 October 2002)

We report on the dynamics of resonant energy transfer in monodisperse, mixed-size, and energy-gradient (layered) assemblies of CdSe nanocrystal quantum dots. Time-resolved and spectrally resolved photoluminescence directly reveals the energy-dependent transfer *rate* of excitons from smaller to larger dots via electrostatic coupling. The data show a rapid (0.7–1.9 ns) energy transfer directly across a large tens-of-meV energy gap (i.e., between dots of disparate size), and suggest that interdot energy transfer can approach picosecond time scales in structurally optimized systems.

DOI: 10.1103/PhysRevLett.89.186802 PACS numbers: 73.63.Kv, 42.70.Nq, 73.21.La, 78.47.+p

Communication, coupling, and coherence between quantum dots are central themes in numerous scientific efforts of present physical and technological interest. Recent realizations of two coupled lithographic quantum dots have shown, e.g., Coulomb blockade [1] and electron pairing [2]. Communication and coherence between several epitaxial quantum dots underpins recent proposals for quantum logic and computation [3,4]. In the limit of large numbers of coupled dots, colloidal semiconductor nanocrystal quantum dots (NQDs) provide a promising route towards large-scale nanoassemblies that can be treated as "artificial solids." In strongly coupled NQD assemblies, electronic excitations can, in principle, delocalize across multiple dots leading to new states described by coherent superpositions of individual dot wave functions. However, coherent coupling requires strong interdot interactions (e.g., electron tunneling) and a high degree of structural order, conditions that are difficult to achieve.

An alternative approach exploits the readily achievable coupling via incoherent long-range dipolar interactions, which allow interdot communication via Förster energy transfer (ET) [5], an effect well known in organic dyes, polymers, and biomolecules [6], and recently observed in NQD assemblies [7] and NQD/dye systems [8]. Here the dipole moment of an exciton in a donor chromophore couples with an absorbing transition in a nearby acceptor, effectively transferring the exciton to the lower-energy chromophore. The Förster ET rate, $\Gamma_{et} = (2\pi/\hbar)J^2\Theta$, depends critically on the spectral overlap integral Θ between normalized donor emission and acceptor absorption line shapes, and on the donor-acceptor Coulomb coupling J, estimated in the dipole approximation as $J^2 = \mu_D^2\mu_A^2\kappa^2/(R_{DA}^6 n^4)$. Here μ_D and μ_A are the donor and acceptor transition dipoles, separated by R_{DA}, κ^2 is an orientational average over all dipoles, and n is the medium's refraction index. In NQD ensembles, where photoluminescence (PL) broadening arises from polydisperse dot sizes, specific spectral components originate from dots of specific size, with smaller (larger) dots emitting towards the blue (red) side of the PL. Thus interdot Förster ET causes an overall PL redshift, and in recent studies of close-packed solids of CdSe and InP NQDs [7], it is largely through these redshifts that the strength and efficiency of the coupling is inferred. Although providing clear evidence for coupling between NQDs, PL redshifts in cw spectra are only indirectly related to the interdot coupling strength. While past studies of NQD solids followed an approach originally proposed for assemblies of organic molecules, a full treatment should include properties particular to colloidal NQDs; namely, that (i) unlike molecules, NQDs have discrete atomiclike energy spectra which hinders the likelihood of donor-acceptor spectral overlap, (ii) the spread of dot sizes precludes the use of inhomogeneously broadened ensemble spectra to calculate spectral overlaps in donor-acceptor pairs, and (iii) nonradiative carrier losses (dominated by surface trapping [9]) are different for each dot, so that PL quantum yield is an ensemble (not single-dot) property.

In this Letter, we directly evaluate the strength of Förster coupling between CdSe NQDs via *dynamical* studies of ET in close-packed assemblies of monodisperse and mixed-size samples, and a prototype "energy gradient" bilayer structure. Through time-resolved and spectrally resolved PL dynamics we observe a fast (0.7 to 1.9 ns) PL decay on the blue side of the emission band which is dominated by Förster transfer, providing a direct measure of ET efficiency. Further, ET proceeds directly from "blue" to "red" sides of the PL band across an energy gap of several tens of meV, i.e., between dots with a relatively large size difference. This observation agrees with the known band-edge structure in CdSe NQDs [10], wherein a large energy gap separates the lowest emitting transition from the higher-lying strongly absorbing transitions. The data suggest that the measured ET rates are limited not by the strength of interdot coupling J, but rather by the low probability of proximal "resonant" acceptors which provide sufficient spectral overlap Θ. Via studies of a prototype energy-gradient structure, and direct comparison with well-known

biological light-harvesting chromophores, we conclude that ET in structurally optimized NQD assemblies can potentially occur on picosecond time scales. These findings reveal the relevant time, size, and energy scales for efficient ET and suggest routes toward engineered design of new NQD assemblies for light-harvesting and directed energy flow.

Colloidal CdSe NQDs with mean radii $R = 11$–22 Å and size dispersion 4%–9% were prepared by organometallic synthesis [11]. We used both as-prepared dots capped with trioctylphosphine oxide (TOPO), and ZnS-overcoated dots for improved surface passivation. Solid-state NQD films 0.2–1 μm thick were drop cast onto glass slides from hexane/octane solutions. Transmission electron microscopy indicates random (amorphous) close packing with average interdot surface-to-surface distances of 11 Å (the length of TOPO). Room-temperature time-resolved PL was acquired via time-correlated single photon counting (35 ps resolution). NQD films were excited at 3.1 eV by 100 fs pulses from a pulse-picked, frequency-doubled Ti:sapphire laser. The pump fluence was $\sim 20\ \mu J/cm^2$, exciting <0.02 excitons per dot on average. Collected PL was dispersed and spectrally selected in a narrow bandwidth (< 1 nm), permitting study of a narrow size range of NQDs.

The inset of Fig. 1(a) shows the PL from a close-packed film of nominally "monodisperse" (7% size dispersion) $R = 12.4$ Å CdSe NQDs overcoated with 9 Å of ZnS (thus, 54 Å between dot centers). This spectrum is redshifted by 35 meV from the spectrum of identical but noninteracting NQDs in solution (dotted line), indicating the presence of ET as observed previously [7]. Here, however, PL decays acquired at the specific energies marked by arrows clearly reveal the energy-, size-, and time-dependent dynamics of interdot ET. On the high-energy side (small dots), the initial PL decay is rapid (1.9 ns). The PL lifetime increases steadily with increasing dot size, reaching a maximum of 22 ns at the lowest energies (largest dots), where the data even show a slight initial increase, indicative of excitons flowing into the larger dots well after the initial excitation. These energy (size) dependent lifetimes unambiguously show direct ET from small to large NQDs, and rule out indirect coupling via photon reabsorption which would not accelerate the decay rate from small NQDs. In contrast, a nearly energy-*independent* 24 ns decay is observed from identical but noninteracting NQDs in solution (dotted line, taken at 2.30 eV). Note that 24 ns is roughly equal to the lifetime of the largest dots in the dense film — this is the intrinsic *radiative* lifetime of excitons in these dots. Note further that all PL decays, even those acquired at high energy, slow down after 10–20 ns and approach this radiative value, indicating that a subset of NQDs (even small ones) do *not* participate in ET, likely due to the absence of proximal resonant acceptor dots, as discussed below. Qualitatively, ET out of the largest NQDs is inhibited by

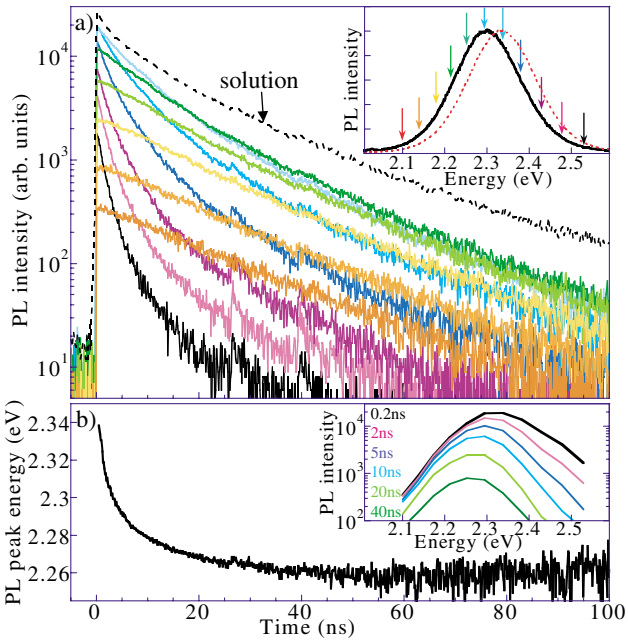

FIG. 1 (color). (a) PL decays from a dense film of monodisperse 12.4 Å CdSe/ZnS NQDs at the energies specified in the inset. Inset: cw PL spectra from film (solid) and original solution (dashed). (b) Dynamic redshift of the peak emission. Inset: PL spectra at the specified times.

the vanishing availability of even-larger dots that can accept excitons. Thus these dots decay radiatively, as in dilute solutions. The faster decays observed from smaller NQDs is due to increased probability of "finding" viable, nearby acceptor dots. The 1.9 ns lifetime from the smallest (bluest) dots is almost entirely due to ET, being over 10 times faster than the (purely radiative) decay of the largest dots.

From these data we derive "instantaneous" spectra to elucidate the *dynamic* PL redshift [Fig. 1(b)]. Initially, the emission is peaked at 2.34 eV, matching that from the NQDs in solution (as expected — this spectrum reflects the actual size distribution of the NQDs). The emission peak redshifts rapidly over the next 10 ns, and beyond 30 ns is roughly constant at 2.26 eV, indicating that ET has effectively ceased — all excitons have migrated to larger dots from which further ET is suppressed. The initial redshift is accompanied by a rapid drop in the *integrated* PL intensity (not shown), which we ascribe to the finite probability for nonradiative deactivation (surface trapping [9]) whenever an exciton transfers to a new dot.

To study the dynamics of ET as proximal dots become disparate in size, we fabricated NQD solids from mixtures of three TOPO-capped CdSe NQD solutions ($R =$ 17, 18, and 21 Å). Figure 2(a) shows the PL from NQD solids of the individual samples, and also from a NQD solid derived from a mixture of the three. Figure 2(b) shows the PL lifetime vs energy in all cases. Efficient ET is seen in the three monodisperse NQD solids, through the

dramatic decrease in PL lifetime from low to high energies within each sample. Here, however, the blue decays are as fast as 700 ps, nearly 3 times faster than in the CdSe/ZnS dots of Fig. 1(a). This faster decay is consistent with the R_{DA}^{-6} dependence of the Förster rate (average center-to-center distance is 47 and 54 Å for TOPO- and ZnS-capped dots). Note also that dots of a particular size which exist in all three samples (e.g., those emitting at 2.175 eV) show completely different dynamics depending on whether they lie on the low-, middle-, or high-energy side of the PL spectrum. When the three sizes of NQDs are combined in solution and cast in a dense "mixed" film, the effects of interdot ET are immediately evident in the PL. While in solution the mixture's PL spectrum approximates the sum of the three constituent PL lines (not shown), the dense film shows a single emission band strongly weighted towards low energies. More interestingly, the PL lifetimes are very short (700–800 ps) throughout the high-energy side, and only at low energies does the lifetime grow, roughly mimicking the behavior seen in the largest of the three NQD samples. Thus for NQDs of a particular size, the rate of ET is due primarily to the availability of nearby viable acceptor dots.

However, in contrast with molecular systems which have broad vibronic homogeneous line shapes, individual NQDs have a discrete atomiclike energy structure, so that "viable acceptors" are not simply all larger nearby dots with lower band gap. Rather, for efficient coupling, a ground-state exciton in a donor dot must be resonant with a strong (but narrow) absorption transition in a nearby dot, implying that only dots which are *larger by a certain amount* are efficient acceptors. This can be qualitatively verified through consideration of the energy-dependent decay rates. Data points in Fig. 3(a) show the decay rates from the data of Fig. 1(a). Using the measured radiative and ET rates $\Gamma_{\text{rad}}^{-1} = 22$ ns and $\Gamma_{et}^{-1} = 1.9$ ns, the dotted line is the calculated decay rate as a function of energy, $\Gamma(\omega)$, assuming that all dots with lower band gap are viable acceptors. Here $\Gamma(\omega) \cong \Gamma_{\text{rad}} + P(\omega)\Gamma_{et}$, where $P(\omega) = \int_0^\omega \phi(\omega')d\omega'$ is the probability that a nearby dot has a smaller band gap and $\phi(\omega')$ is the normalized size distribution of the NQD ensemble, equivalent to the PL spectrum in solution. While reproducing the experimentally observed trend, the curve is clearly redshifted from the data. However, if we permit as viable acceptors only those dots which have a band gap smaller *by at least 55 meV* [see inset, Fig. 3(a)], the calculated curve matches the data remarkably well. This strongly suggests that in this sample, efficient ET occurs primarily between NQDs having a significant band gap energy difference, i.e., between NQDs of markedly different size.

The above conclusion is reassuringly consistent with the energy structure of NQD band-edge exciton states theoretically predicted and experimentally analyzed in detail [10]. Within the effective-mass model, the lowest exciton state in CdSe NQDs consists of lower and upper manifolds of closely spaced levels. The lower exciton manifold from which PL emission occurs has a relatively weak oscillator strength, whereas the upper manifold is characterized by a much stronger transition observed as the intense (1S) absorption peak in ensemble spectra. The energy gap between lower and upper exciton manifolds is observed in optical spectra as a size-dependent, tens-of-meV "global Stokes shift" between absorption and emission peaks. Thus *optimal* ET occurs when the emitting/absorbing transitions in donor/acceptor pairs are resonant [Fig. 3(b)]. The transferred exciton then relaxes on sub-ps times to the acceptor's ground state [9]; in this way

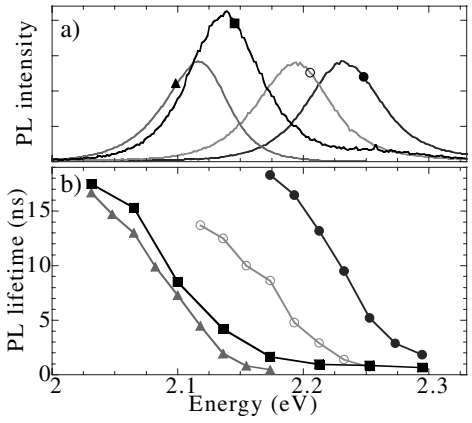

FIG. 2. (a) cw PL from films of 17, 18, and 21 Å CdSe NQDs, and from an equal mixture of the three (squares). (b) Corresponding PL lifetimes vs energy.

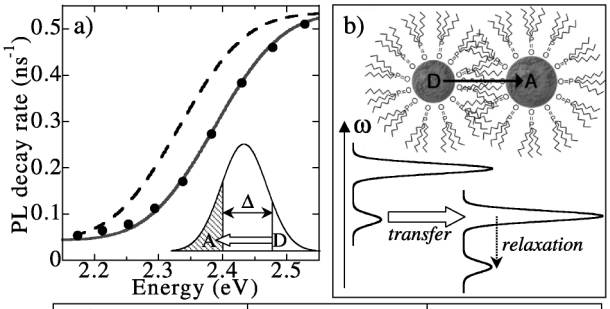

c)	resonant NQDs	LH2 [Ref.12]
Dipole μ_A (μ_D)	25 (4.4) Debye	8.2 (8.2) D
Distance R_{DA}	54 A	18 A
Coupling J	2.4 cm^{-1}	26 cm^{-1}
Overlap integral Θ	0.004 cm	0.0004 cm
Estimated rate Γ_{et}	(38 ps)$^{-1}$	(3 ps)$^{-1}$

FIG. 3. (a) Calculated decay rate vs energy with no gap (dashed) and 55 meV gap (solid) between donor and acceptor. Points are measured data. (b) "Resonant" ET; interpenetrating TOPO caps give ~11 Å dot spacing (not to scale). (c) Typical Förster parameters for resonant NQDs, and for B800-B850 transfer in LH2 complex of purple bacteria. NQD values based on measured radiative lifetime (22 ns), assumption of 20 meV homogeneous linewidths at 300 K, and calculated oscillator strengths from Ref. [10], using $n = 1$ and $\kappa^2 = 2/3$.

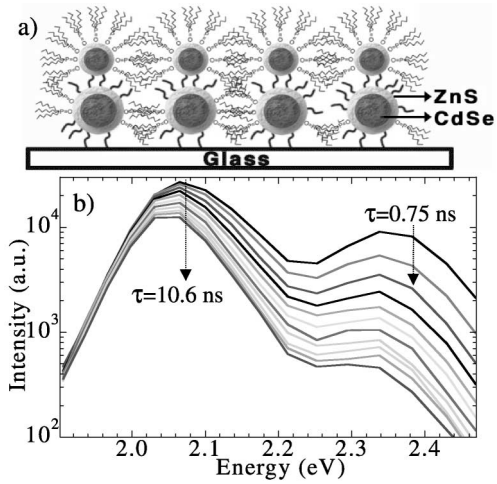

FIG. 4. (a) Schematic of NQD energy-gradient bilayer for light harvesting—13 Å dots on 20.5 Å dots. (b) "Instantaneous" PL spectra at 500 ps intervals (from 0 to 5 ns), showing rapid collapse of emission from 13 Å dots.

excitons transfer directly and irreversibly from blue to red sides of the PL spectrum.

The ET rate between optimally resonant donor-acceptor NQD pairs may be estimated via direct comparison with well-studied biological light-harvesting (LH) complexes, such as the two coupled chlorophylls in the LH2 antenna complex of photosynthetic bacteria. Figure 3(c) lists typical parameters for LH2 [12] and for the CdSe/ZnS dots of Fig. 1(a). In NQDs, the Förster ET rate, averaged over dipole orientation, is estimated to be as fast as ~38 ps—far faster than the measured 1.9 ns. This marked contrast highlights the primary bottleneck to fast ET in NQD solids: Because of the narrow linewidths of individual NQD spectra and the inhomogeneous distribution of NQD sizes, the probability of finding a nearby acceptor with appreciable spectral overlap Θ is small. In fact, only when considering coupling to *next-nearest* neighbors ($R_{DA}^{nnn} = 2R_{DA}$) do the estimated values approach nanosecond time scales, suggesting that observed dynamics in close-packed monodisperse and mixed 3D solids may, in fact, be dominated by ET to one or more acceptors in the *second* shell of dots.

For the monodisperse and mixed NQD assemblies discussed thus far, we expect a random occurrence of optimally resonant donor/acceptor pairs. In a final experiment, we attempt to artificially engineer the incidence of efficient Förster ET, with an aim towards boosting the rate of ET closer to the estimated limit, and generate directed energy flows in artificial materials. We fabricated a prototype bilayer light-harvesting NQD structure from monolayer-by-monolayer assembly of $R = 13$ Å CdSe/ZnS dots on 20.5 Å dots [Fig. 4(a)]. The substrate is silanized with thiol-functionalized "anchor" molecules that bind the large dots, which are then derivatized with dithiol linkers to promote covalent binding of the second (small) dot layer [13]. The distance between small and large dot centers is $R_{DA} \simeq 62$ Å. Here the size disparity is large, so that coupling of donor excitons to the dense manifold of higher-lying excited states in large dots is possible, effectively guaranteeing improved spectral overlap between small and large dots. Instantaneous PL spectra [Fig. 4(b)] reveal the nearly complete depletion of excitons from the 13 Å dots within 5 ns, but only a small decrease in the large NQDs, indicating efficient ET from small to large dots in the vertical direction (in solution, both small and large dots exhibit long ~20 ns decays). PL decays from the small dots are very rapid (750 ps), which is over twice as fast compared to the monodisperse CdSe/ZnS NQD solid of Fig. 1, despite a larger interdot separation ($R_{DA} = 62$ vs 54 Å), and a much smaller number of possible neighbors due to the 2D bilayer nature of the structure. Thus by ensuring donor/acceptor spectral overlap, and intentionally placing acceptors near donor dots, the rate of ET is enhanced, and the direction of energy flow can be influenced.

Based on these findings, we anticipate that further improvements in size selectivity, PL quantum yield, and controlled growth of NQD "artificial solids" will permit highly efficient and engineered energy flows in tailor-made NQD assemblies, with exciton transfer potentially approaching the tens-of-ps time scales estimated above. A promising aspect of NQDs are the long (> 20 ns) intrinsic exciton lifetimes, so that even with a 750 ps Förster ET time, an exciton could, on average, migrate over 25 times before recombining in an appropriate structure wherein sufficient layers of carefully size-selected dots are stacked in an energy-gradient fashion. This estimate further highlights the importance of good NQD surface passivation to suppress surface trapping, a principle mechanism for exciton nonradiative losses.

This work was supported by Los Alamos LDRD funds.

[1] C. Livermore *et al.*, Science **274**, 1332 (1996).
[2] M. Brodsky *et al.*, Phys. Rev. Lett. **85**, 2356 (2000).
[3] A. Imamoglu *et al.*, Phys. Rev. Lett. **83**, 4204 (1999).
[4] E. Biolatti *et al.*, Phys. Rev. Lett. **85**, 5647 (2000).
[5] T. Forster, Naturwissenschaften **33**, 166 (1946).
[6] A. Dogariu *et al.*, Synth. Met. **100**, 95 (1999).
[7] C. R. Kagan *et al.*, Phys. Rev. Lett. **76**, 1517 (1996); O. I. Micic *et al.*, J. Phys. Chem. B **102**, 9791 (1998).
[8] C. E. Finlayson, D. S. Ginger, and N. C. Greenham, Chem. Phys. Lett. **338**, 83 (2001).
[9] V. I. Klimov, J. Phys. Chem. B **104**, 6112 (2000).
[10] A. L. Efros *et al.*, Phys. Rev. B **54**, 4843 (1996).
[11] C. B. Murray, D. J. Norris, and M. G. Bawendi, J. Am. Chem. Soc. **115**, 8706 (1993).
[12] V. Sundstrom *et al.*, J. Phys. Chem. B **103**, 2327 (1999).
[13] J.-Y. Tseng, M.-H. Lin, and L.-K. Chau, Colloids Surf. A **182**, 239 (2001).